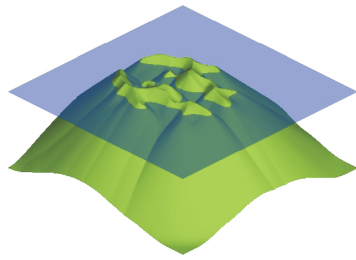
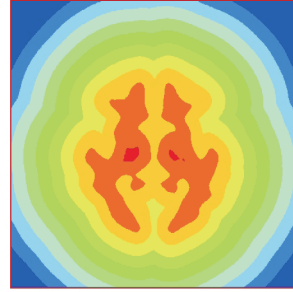


CHAPTER 11: J-DIVERGENCE BASED ACTIVE CONTOUR MODELS



(a) Level set function in 3D



(b) Color representation of distance function

Figure 1. (a) Representation in three dimensions of the intersection of a level set with the zero plane. (b) Color contour of the level set function in (a). Colors represent the Euclidean distance.

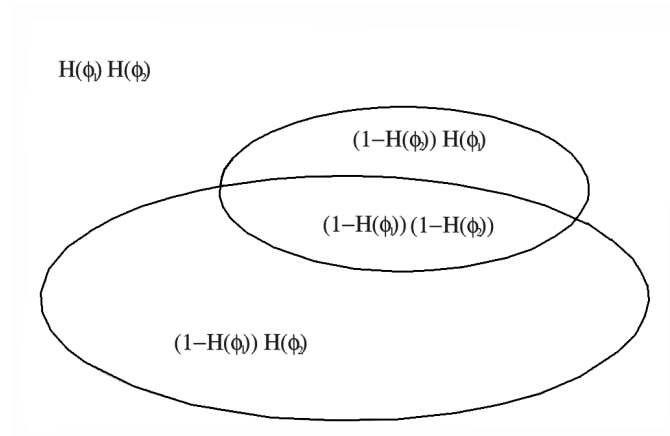


Figure 2. Four-phase level set model illustration. There are four regions in the image, using two level set functions. They can be represented by $H(\phi_1)H(\phi_2)$, $(1 - H(\phi_1))H(\phi_2)$, $H(\phi_1)(1 - H(\phi_2))$ and $(1 - H(\phi_1))(1 - H(\phi_2))$.

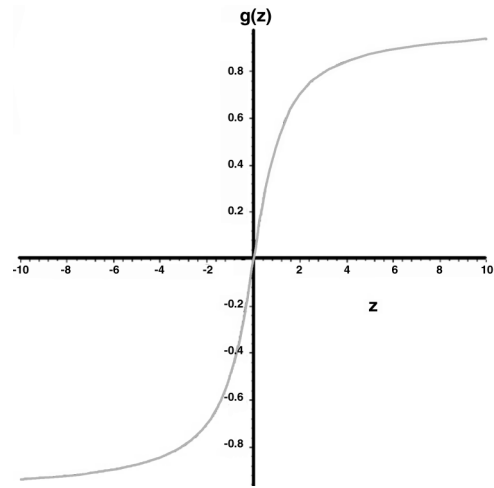


Figure 3. Normalized velocity.

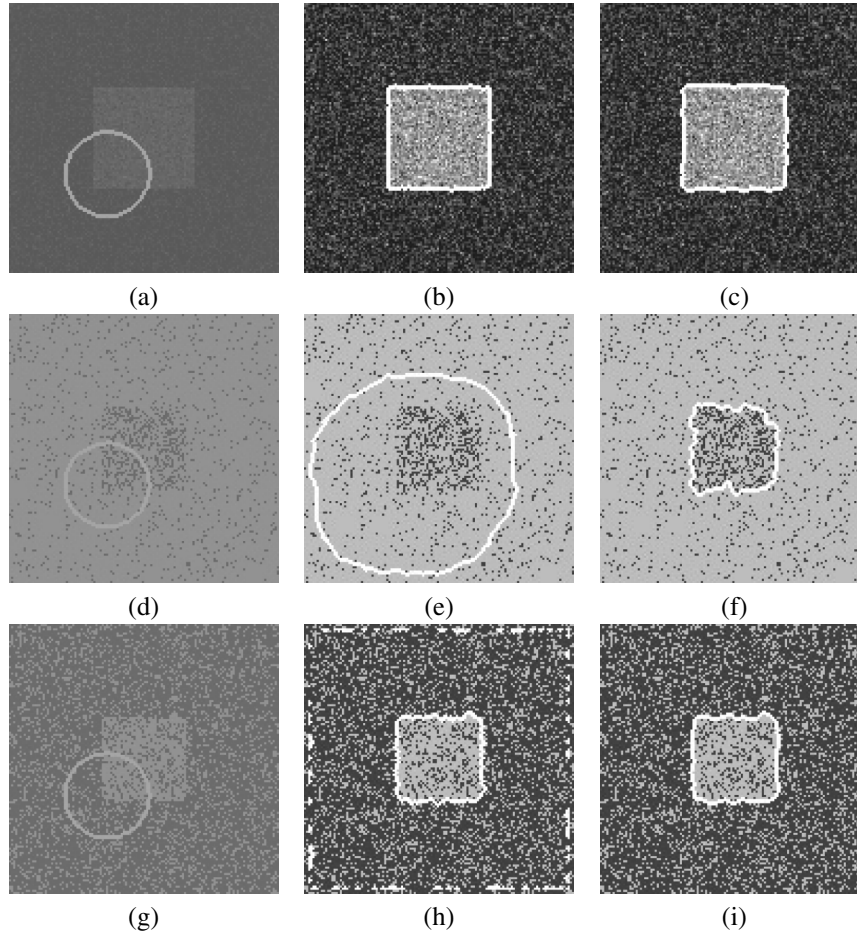


Figure 4. Segmentation of a square pattern from background. The first row shows initializations for both algorithms. The second row shows the results of geodesic active regions [11, 12, 13]. The third row shows results of the proposed algorithm. (a-c): Gaussian noise, background mean/variance = 10/100, square mean/variance = 10/225. (d-f): Gaussian noise, background mean/variance = 0/0.1, square mean/variance = 0/1 (the curve in (e) will not stop and expands out of the image domain). (g-i): salt and pepper noise, background and square mean = 1 noise density = 0.5.

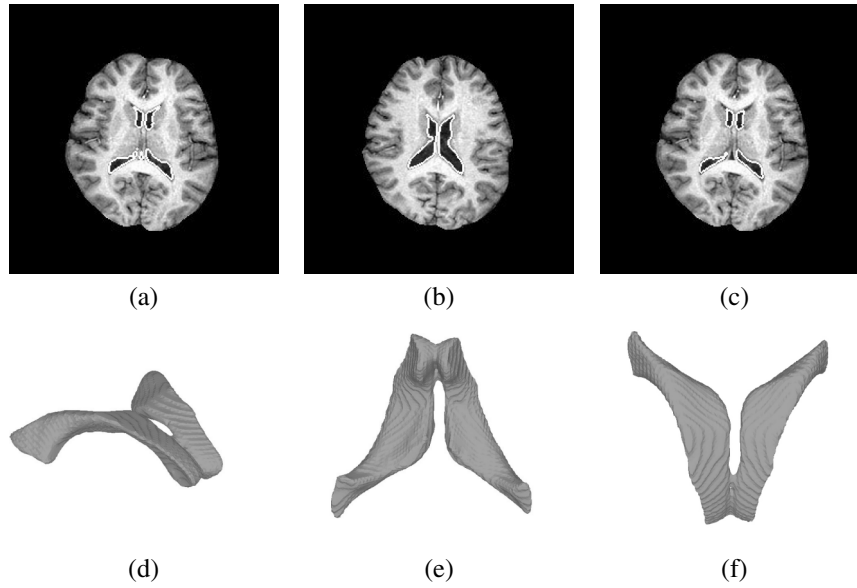


Figure 5. Segmentation of lateral ventricles from MRI brain data: (a–c) final contour in different axial slices; (d–f) segmentation results represented by a 3D surface.

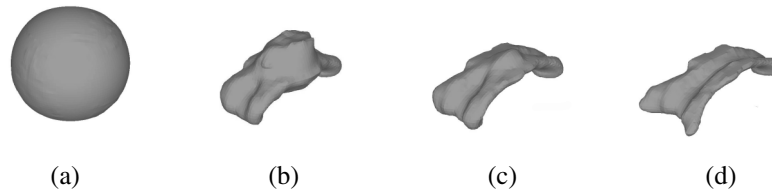


Figure 6. Segmentation of corpus callosum from 3D DTI data: (a) initial surface, a sphere; (b, c) intermediate evolution results; (d) final result.

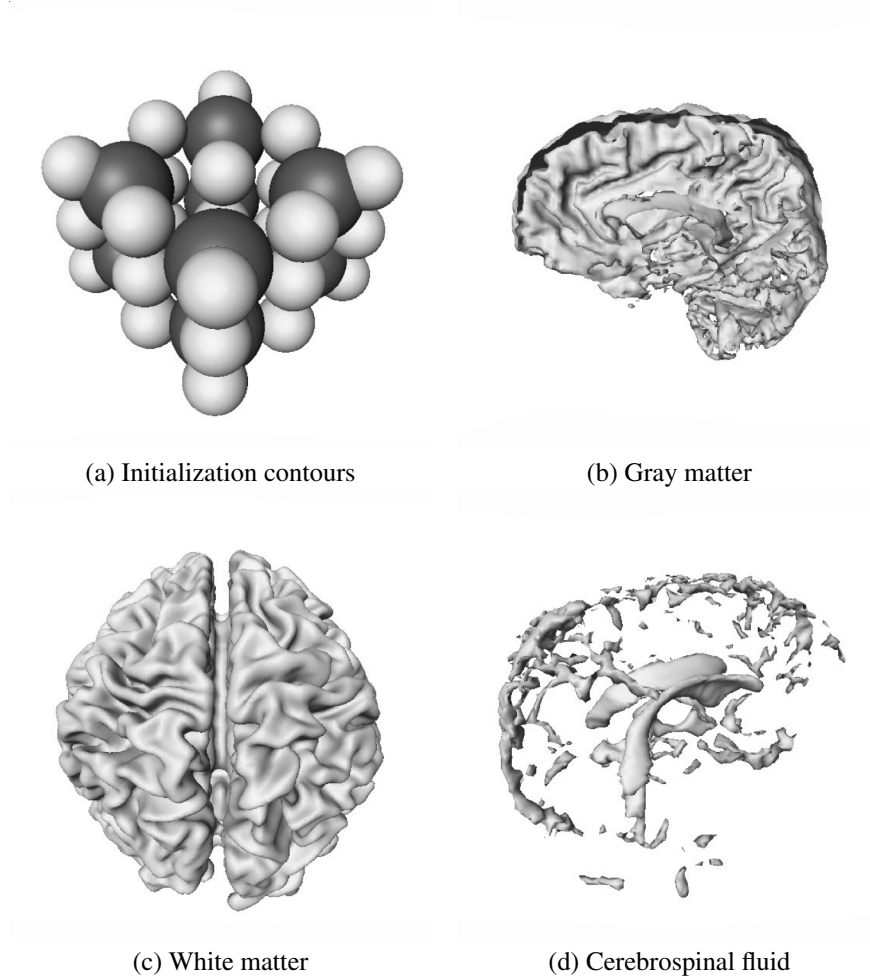


Figure 7. 3D MRI segmentation using three-phase level set model: (a) initial surface; 27 small spheres are initialized for ϕ_0 , 4 larger spheres are initialized for ϕ_1 ; (b) final GM segmentation result; (c) final WM segmentation result; (d) final CSF segmentation result.